Photochemistry of CH 3 I×××(H 2 O) n Complexes: From CH 3 I×××H 2 O to CH 3 I in Interaction with Water Ices and Atmospheric Implications

Sophie Sobanska, Michelle Custodio-Castro, Rosana Romano, Joëlle Mascetti, Stéphane Coussan

UV Photochemistry of $CH_3I...(H_2O)_n$ complexes. From $CH_3I...H_2O$ to CH_3I in interaction with amorphous, cubic and hexagonal water ices and atmospheric implications

Sophie Sobanska,*,† Rosana M. Romano,‡ Michelle T. Custodio-Castro,‡ Joëlle Mascetti,† and Stéphane Coussan*,¶

†*Institut des Sciences Moléculaires, Université de Bordeaux 1, CNRS UMR 5255, Talence, France.*

‡*CEQUINOR (UNLP – CONICET, CCT La Plata, associated with CIC PBA). Departamento de Química, Facultad de Ciencias Exactas, Universidad Nacional de La Plata, Boulevard 120 e/ 60 y 64 No 1465, La Plata (CP 1900), Argentina.*

¶*Aix-Marseille Univ, CNRS, PIIM, Marseille, France*

E-mail: sophie.sobanska@u-bordeaux.fr; stephane.coussan@univ-amu.fr

Abstract

The broad band UV photochemistry of CH_3I trapped at the surface of amorphous, cubic and hexagonal ices have been studied by FTIR spectroscopy. Those results have been compared with UV broad-band photochemistry of CH_3I bare monomer and complexed with water, trapped in argon cryogenic matrices. We also studied the effect of heating the ice on CH_3I desorption. These effects clearly highlight the difference in CH_3I behaviour depending on the trapping sites. It appears that if CH_3I interacts with

water molecules (in the matrix) or water ice by hydrogen bonding, then CH_3I does not fragment under UV irradiation. Thus, the energy transfer to the network of hydrogen bonds in the ice or matrix is effective. On the other hand, to a first approximation, if CH_3I interacts by picnogen-type bonding, then CH_3I fragments, because in this case the electronic relaxation seems to take place mainly at the intramolecular levels of CH_3I. These effects are of a prior interest in understanding their ageing processes (mainly hydration and UV-photochemistry), especially in the Earth's atmosphere physical chemistry context. Indeed, iodomethane which is a natural product emitted in really weak amount by algae and micro-algae at the surface of seas and oceans, can be emitted in a large amount in case of a severe nuclear accident (Fukushima and Chernobyl). In this latter case, iodomethane will be radioactive, while being already an alkylating agent that can damage DNA. During this ageing process reactions occur which could lead to CH_3I fragmentation along C-I bond. One of the products is I_2 easy to absorb by human body. It is thus important to guess, already at the molecular level, what is the fate of iodomethane in interaction or not with water or water ice, two of the most abundant Earth's atmosphere chemical components, upon UV irradiation.

Introduction

Atmospheric halogen chemistry has received extended attention, as the emission of halocarbons into the troposphere may play an important role in stratospheric ozone depletion, change the tropospheric oxidative capacity and in the formation of ultrafine aerosols. Iodine photochemistry decreases the tropospheric O_3 burden more efficiently than chlorine (on per atom basis), decreasing radiative forcing[1,2] and reduces the atmospheric OH burden, increasing the lifetime of greenhouse gases.[3] Iodine may also dominate new particle formation and particle growth in coastal area[4,5] and in artic.[6] Iodine compounds are naturally released mainly from the oceans either by marine metabolisms (i.e. phytoplankton and micro- and macro-algae) or, in the case of inorganic iodine species (HOI and I_2), result from the reac-

tion between O_3 and iodide in seawater ([11–15] reviewed by Carpenter *et al*[16]). Terrestrial sources of iodine species from arid regions are much less important than marine sources, but have been identified as significant O_3 sinks.[17] The measurements performed during field campaigns showed that photochemical processes occurring within the snowpack may alter the atmospheric composition including the iodocarbon content.[18,19] The discovery of primarily methyl iodide (CH_3I) as potential sources of reactive halogen species during ozone depletion processes[20] have motivated investigations of photodissociation of CH_3I adsorbed on ice.[9,10,21]There have been extensive experimental and theoretical studies on the photodissociation of CH_3I in the gas phase[22–26] or adsorbed on ice surfaces.[21] In gas phase,[22–26] decomposition along C-I bond ($\sigma^* \leftarrow n$) leading to different photoproducts including I_2. The CH_3I A-band (210-350 nm)[22] contains five transitions: two forbidden, $^3Q_2(1E)$ and $^3Q_{0-}(1A_2)$; one strong parallel repulsive, $^3Q_{0+}(2A_1)$; and two perpendicular weakly repulsive, $^1Q_1$ and $^3Q_1$.[22] The dynamics of the A-band ultraviolet photodissociation of methyl iodide has been experimentally explored at 304 nm,[22] at 240 and 260 nm,[25] or 255 and 269 nm[26] (this list being not exhaustive), by several techniques. It appears that depending on the irrradiation wavelength, a subtle and complex electronic relaxation takes place, leading at the end to, among others, iodine in its excited state $I^*(^2P_{1/2})$ or in its ground state $I(^2P_{3/2})$, ultimately giving the I_2 molecule. Orlando *et al*,[21] worked on CH_3I UV photodissociation at ASW surface, irradiating at 260 and 290 nm. They concluded that I_2 can be formed and ejected if iodine is in its $I^*(^2P_{1/2})$ excited state and that prior to this formation, $(CH_3I)_2$ is present in the gas phase.

Ice in natural environment may exist with various crystalline forms including hexagonal (Ih) and cubic (Ic) symetries.[27] Ice that grows under vacuum conditions (*i.e.* $P < 10^{-6}$ mbar) could exist under several different forms depending on the cold substrate temperature. The deposition of water vapor at substrate temperatures below 110 K results in the formation of low-density porous amorphous solid water (PASW, hereafter referred as ASW), while at higher temperatures (>130 K) one observes the formation of mainly two types of crystalline

ice: cubic (140 K)(hereafter referred as Ic) and hexagonal (170 K) (hereafter referred as Ih). At the molecular scale, ASW presents special surface molecules with dangling modes able to accrete small molecules such as CO, H_2, O_2, N_2, CO_2 ... to CH_3OH(Fig. 1),[28,29] what could induce further chemical and/or photochemical reactivity.[30] However, the adsorption, desorption and UV photochemistry of CH_3I, trapped on the surfaces of ASW, Ic and Ih water ices, to explore the effect trapping sites on the UV photochemistry of CH_3I or on desorption by global heating of the substrate has not been explored. The fundamental questions are: *(i)* the way water ice is able to dissipate IR or UV-visible energy, absorbed directly through surface modes,[30–32] or through bulk ones.[33] *(ii)* The way water ice is able to relax UV energy acquired through the adsorbat, iodomethane. What will be the effect of this dissipation? Desorption, fragmentation, surface reconstruction or partial melting ...? We addressed all these questions in this work trying to establish a link between purely physico-chemical data, at the molecular level, and atmospheric implications.

Matrices and Ices Experiments

Gaseous samples of CH_3I/Ar (0.1% CH_3I - 99.9% Ar, Airproduct) were used without any further purification. For matrix experiments, we used this latter mixture, *i.e.* a ratio of CH_3I/Ar $\approx$ 1/1000, while with water we used a ratio of $H_2O/CH_3I/Ar \approx 1.5/1/1000$. Matrices were deposited by one 10s pulse (1bar in the mixture ramp) on the sample carrier maintained at 20 K. The samples were then cooled down to 4.3 K. ASW samples were prepared as follows: deionized water was subjected to multiple freeze-pump-thaw cycles under vacuum to remove dissolved gases. Mixtures of purified H_2O and helium (Air Liquide, 99.9999%) gas were prepared in a ramp with a base pressure of 10^{-4} mbar at a ratio of H_2O:He = 1:25. Ices were produced by depositing the gas mixture directly onto a gold-plated copper surface held at 50 K (to avoid trapping of the vector gas or residual nitrogen[30]) then cooled to 3.7 K (the cooling typically takes around 5 min due to the high power of the cryogenerator (PT-405

Cryomech, 0.5 W at 4 K)). Ic and Ih ices were obtained, under 10^{-7} mbar vaccuum, by annealing ASW to 140 K and 170 K, respectively. CH_3I/Ar mixture was deposited on ASW, or crystalline ices (Ic and Ih), by one injection of 10 s (mixture pressure $\approx$ 1 bar), at 50 K in order to not trap Ar. The samples were then cooled down to 4.3 K.IR spectra were recorded in reflection mode using a Bruker 66/S FTIR spectrometer equipped with a KBr/Ge beamsplitter and a MCT detector (4000-800 cm^{-1}, 0.12 cm^{-1} resolution, 50 or 100 scans). For matrix isolation experiments CH_3I/Ar mixture has been deposited by pulsed deposition (Parker electromagnetic valve), onto the gold-platted copper cube cooled to 20 K. Cryostat and sample-carrier were protected from thermal background radiation by a chrome-platted brass shield. Controlled heating (Lakeshore Model 336) of the sample carrier was carried out with a 50 Ω resistor, while the background pressure in the vacuum chamber was kept at 10^{-7} mbar by a turbomolecular pump. Broad band UV irradiation were carried out with an Oriel high-pressure mercury lamp (average power: 600 mW, no water filter) with a high-pass 290 nm or without optical filters. Typically we irradiated tens of minutes with and without high-pass filter. We irradiated untill we reached the photo-equilibrium.
All experiments were performed at least twice under exactly the same conditions.

Results and Discussion

In our previous work on $CH_3I...(H_2O)_n$ complexes and aggregates trapped in argon cryogenic matrices, we observed some mixed aggregates and complexes, but the main phenomenon was the auto-aggregation of each of those molecules.[36] As a conclusion, especially in the event of a nuclear major accident, the spreading of radioactive iodomethane through an association with water, is unlikely. However, Earth's atmosphere contains also water ice which is able to trap at its surface (ASW, Ic and Ih) but also in pores (ASW),[28] a considerable quantity of iodomethane. Indeed, in the case of adsorption of small molecules on amorphous ice, including methane, Roubin *et al*[29] gave a specific area of $\approx 100\,m^2\,g^{-1}$ while Loerting *et al*,[37] give a specific area comprised between <0.1 to 280 $m^2\,g^{-1}$. There is no comparison between

a complex water/iodomethane and a solid able to offer $\approx 100\,m^2\,g^{-1}$ to adsorption, as ASW. It means, in a first rough approximation, that if we consider CH_3I as a hard sphere, its 2D representation at the surface of ice will be a disk of πR_w^2 area (R_w is the Van der Waals radius; 198 pm for CH_3I), *c.a.* 12.3 Å^2 per molecule. It leads, if we consider uniquely the first monolayer, to a possible capture of $\approx 81.10^9$ molecules of CH_3I per gram of ASW, a complete change of scale.

Differences between ASW (top spectra), Ic (medium spectra) and Ih (bottom spectra) are clearly observable in Figure 2. These ices have characteristic band shapes in the νOH region. As can be seen, the transition from amorphous to crystalline ices is accompanied by a structuring of the bulk band and a decrease in the FWHM (Full Width at Half Maximum). This effect is due to the organization of the material, which reduces the number of oscillator classes. This implies changes both in the bulk and at the surface. During this transition from amorphous to crystalline ice, the dH modes (Figure 1) flip towards the bulk. The consequence is that only dO and s4 type water molecules remain at the surface. This reduces the possibility of aggregation of the adsorbates.

As can be seen in Figure 2 and Table 1, whatever the type of ice, we observe CH_3I trapping, almost at the same positions, excepted in the νOH region, in which because of dH modes flipping toward the bulk (Ic and Ih), only trapping at "dO and s4" type positions can be observed. Since we are no longer dealing with amorphous ice, these surface modes are of the "dO and s4" type, but for ease of reference we will call them dO and s4. The fact that we can call the surface molecules, in the case of Ic and Ih ices, dO and s4, as in the case of amorphous ice, is strongly supported by the fact that trapping frequencies are almost the same (*i.e.* perturbations are comparable, then geometries of those surface cristalline ice molecules are comparable with those dO and s4 of ASW). More surprisingly, the characteristic frequencies of the ν_{CH} and δ_{CH} modes for CH_3I monomer trapped in argon matrix appear to be in virtually the same position as for CH_3I monomer trapped on the surface of the different ices (Figures 3, 4 and 5). On the other hand, when CH_3I interacts with water

in argon matrix (Figure 5, spectra e), we observe almost the same δ_{CH} positions as those on ice, for the monomer, while hydrated complexes multiplet is blue-shifted, with respect to that of the monomer, from 1245 cm^{-1} to 1254 cm^{-1} (average frequencies). In the same way, ν_{CH} mode is blue-shifted from 2871 to 2962 cm^{-1} (a weak band is nevertheless observed at 2960 cm^{-1} in bare iodomethane in argon matrix). We can then clearly discriminate between a hydrated iodomethane complex and iodomethane monomer in interaction with cyrogenic solids, argon matrix, or water ices.

The global warming effects of ASW after iodomethane trapping is presented in Figure 6. We study those effects on ASW, because this is the only one which presents the four surface oscillators presented in Figure 1. Indeed, because of their crytalline structures, cubic, Ic, or hexagonal, Ih, ices present no dH oscillators. It reduces thus adsorption capacity. From the difference spectrum labelled (e), obtained after annealing at 70 K, we can see that the main desorptions take place at the frequency of 3682.7 cm^{-1}, *i.e.* the danglings dH. At the same time, no significant changes in ν_{CH} and δ_{CH} domains are observed. As for the ice, it has already begun to restructure, as evidenced by the movements observed in the bulk. Looking at the warming at 130 K (spectra c and f), it is clear that this time, dO and s4 sites show the strongest decreases, and therefore certainly the strongest desorptions. We can also see that in this case a response is also observed in the ν_{CH} and δ_{CH} zone. Finally, when heated to 150 K (spectra d and g), the ice crystallised as Ic, and all the iodomethane has desorbed. However, these results should not lead to any conclusions about the binding energy of molecules trapped at dH sites compared to those at dO and s4 sites. This is all the more true because at 70 K, the ice has already begun to restructure, leading to the tilting of a certain number of dH sites, certainly accompanied by the desorption of the CH_3I trapped on them. On the other hand, what is more interesting in terms of the difference in geometry, is the fact that we do not observe any change in the ν_{CH} and δ_{CH} zone during the desorption of the molecules trapped on the dH. Since we cannot postulate that there is less iodomethane trapped on dH

than on dO and s4, this difference in intensity is directly linked to a difference in trapping geometry. Indeed, intensity of an absorption band cannot be easily linked to the quantity of molecules trapped, while it is directly linked to the derivative of molecular dipole moment with respect to normal coordinates, thus to geometry. In the present case, it is accompanied by low intensities (as calculated in the case of the bare iodomethane molecule[36]) for the molecules trapped on dH and, on the other hand, by an increase in these signals for those on dO and s4 (Figure 7). In other words, molecules trapped on dH sites obviously show ν_{CH}/δ_{CH} signatures, but with intensities so low that no trace of desorption can be detected by heating to 70 K.

If we now turn our attention to the effects of broadband UV irradiation, with and without a high-pass filter ($\lambda > 290$ nm, to mimic solar radiation), we identify differents effects. As can be read in the captions of the Figures 2 to 5, we both irradiate, in the same series, with the high-pass filter ($\lambda > 290$ nm) and then without. In both cases we observe the same effects, but really limited in the case of the high-pass filter irradiation. This is easy to understand because, as mentioned above, iodomethane presents five transitions in its A-band, the most intense of which is $^3Q_0$ located below 290 nm. Above this former wavelength, there remains the $^3Q_1$, which is the weakest, directly involved in this "UV-high-pass filter" photochemistry (that mimics sun irradiation).[22,25,26] The main observed effects are a decrease in the ν_{OH} region located at $\approx$ 3607 cm^{-1}, in the ν_{CH} one at 2943 cm^{-1} and then at 1431, 1401 and 1241.8 cm^{-1}, in the δ_{CH} one, respectively. In the other hand, one can observe that at 3682 cm^{-1}, *i.e.* dH position, there is no change. A first conclusion is that iodomethane molecules trapped on dH positions do not fragment upon UV irradiation while those trapped on dO or s4 do. Another point which should be noted is that we systematically observed the same kinetics whatever the type of ice or of molecule: bare iodomethane, or associated with water, trapped in argon matrices. So, it is obvious that water ice does not catalyse iodomethane fragmentation. When we talk about the catalytic effect of ice on CH_3I fragmentation, we are

talking about two things. The first is that it is not the trapping on the ice surface that causes CH_3I fragmentation. The proof is that we also observe this fragmentation in the matrix, and that it is observed in the gas[24–26] phase. Similarly, even if the irradiation times are not exactly the same for different ices or matrices, they can be counted in tens of minutes. Given this, and the weakness of the UV[24–26] absorption bands, it is very difficult to speak of a catalytic effect of the ice on this fragmentation. In our experiments, by varying the irradiation times at the same power, we always observed the same kinetics, whatever the ice. The key question is, in very simplified terms, with "how many" water molecules does the iodomethane monomer interact? Indeed, in matrix experiments, in excess of water (Figure 4, bottom spectra), it appears that CH_3I fragmentation is greatly reduced, even non-existent. In fact, in the ν_{CH} zone there is virtually no CH_3I fragment generation. In this case, the water causes a change in the electronic relaxation path and certainly favors the transfer of excess energy or to the matrix, or to the water complexes in the close neighborhood of iodomethane monomer, or in interaction with it, and then to the matrix. We can then easily transfer this reasoning to iodomethane in interaction with ice. We remind here that excepted $CH_3I...OH_2$,)**1wb** hetero-dimer, Figure 7),[36] all the other species identified in argon matrix are H-bonded. Contrary to what we observed for namely pyridine-water dimers trapped in cryogenic matrices,[38] in which water is a "spectator" partner, here water is the key of CH_3I electronic relaxation (this fact is strongly supported by the observed CH_3I fragmentation in argon matrix when there is no water (Figure 4, top spectra)). As already described in litterature,[22,25,26] iodomethane decomposition along C-I bond ($\sigma^* \leftarrow n$) will lead to CH_3 and I fragments, as can be seen in the ν_{CH} region (Figures 3 and 5), which will evolve in turn. Concerning dH trapped iodomethane monomer, UV irradiation does not involve neither fragmentation, nor desorption. This fact can be understood in terms of electronic relaxation paths and coupling with reaction coordinates that can lead to fragmentation or desorption. As reported in the literature, a wide range of irradiation wavelengths have been tested on iodomethane. All of them lead to its fragmentation via different pathways depending on

the couplings between electronic states. The fact that the dH modes of the ASW in the case of trapped iodomethane prove that the seat of relaxation is not CH_3I, but that there has been a transfer to the hydrogen bonding network of the amorphous ice, which is able to dissipate this excess energy (as in the case of iodomethane-water complexes in matrices reported above). In the case of the monomers trapped on dO and s4, the site is now, even if this does not concern all the molecules trapped on these sites. In fact, as can be seen from the Figures 2 to 5, the fragmentation affects only a part of the population trapped on the latter, and perhaps also desorption, but without a mass spectrometer it is difficult to say. Can these observations be linked to the geometry of the "local complexes" created by trapping at the dH, dO and s4 sites? And can we, as a first rough approximation, compare them with the geometries of the $CH_3I...H_2O$ complexes calculated in our previous work[36] (Figure 7)? If we look at the two forms **1wa** and **1wb** in Figure 7, the former seems to be more suitable for trapping at dH sites, while the latter seems to be more suitable for trapping at dO and s4 sites. Does this mean that the transfer of energy to the ice lattice, whatever it may be, is more efficient through hydrogen bonds than through picnogen (I...O) bonds? Given the current state of knowledge and the approximations of these calculations performed for only isolated species, this remains a hypothesis.

Conclusion and Perspectives

In this paper, we have described a detailed study of the UV photochemistry of iodomethane monomer trapped in argon matrix or on the surface of amorphous and crystalline water ice. We have also studied the UV photochemistry of iodomethane-water complexes trapped in an argon matrix. The aim of this study is to gain a better understanding of the fate of the emitted iodomethane in the context of atmospheric physico-chemistry and, more specifically, of a major nuclear accident, *i.e.* its atmospheric transport, but also its ageing by hydration or capture by atmospheric ice, combined with the effects of solar radiation. It appears that when CH_3I is adsorbed on the surface of amorphous, ASW, or crystalline, cubic, Ic, or

hexagonal, Ih, water ice, its behaviour under UV irradiation or by heating the ice differs according to the trapping sites. When CH_3I interacts with water ice by hydrogen bonding, no fragmentation is observed during UV irradiation on the dH dangling modes, whereas this partial fragmentation (the entire population of these molecules is not fragmented) is observed on the dO and s4 positions. Similarly, in the matrix, the CH_3I monomer is fragmented by UV irradiation, whereas when it is associated with water by hydrogen bonding, this fragmentation seems to be almost 'quenched'. Can we relate this phenomenon to the modes of interaction between iodomethane and atmospheric water molecules or water ice? Indeed, it seems that interaction by hydrogen bonding facilitates the transfer of energy during electronic relaxation to the matrix or network of hydrogen bonds in the bulk of amorphous water ice. Conversely, a picnogen interaction between iodomethane and water or the surface of amorphous or crystalline ice seems to cause the fragmentation of iodomethane. The latter seems to be the preferred case, where the fragmentation of CH_3I can yield halogenated alkyl by-products, or I_2. Consequently, depending on the type of association with water or the adsorption sites on ice, CH_3I does not show the same evolution under UV irradiation. On the other hand, contrary to what has been reported in the literature, ice does not catalyse the photofragmentation of CH_3I. Rather, it modifies the electronic relaxation paths, some of which lead to the fragmentation of iodomethane. One of the prospects of this work is to pursue the same type of study on other halogenated methyl compounds such as, CH_3Br and CH_3Cl.

Acknowlegdments

The authors thank Christian Aupetit, from ISM laboratory in Bordeaux, for its technical support. Authors thanks ECOS program (n° A18ST03) for financial support.

Table 1: Experimental OH frequencies of adsorption sites of CH_3I, on ASW, Ic and Ih ices. [a]Ref 15. n.o.: not observed. [b] on ASW; [c] on Ic and Ih

Sites	bare ASW[a]	bare Ic	bare Ih	Adsorbed CH_3I
dH	3720			3682[b]
dH	3698			3682[b]
dO	3549	n.o.	n.o.	3607[b,c]
s4	3503	n.o.	n.o.	3607[b,c]

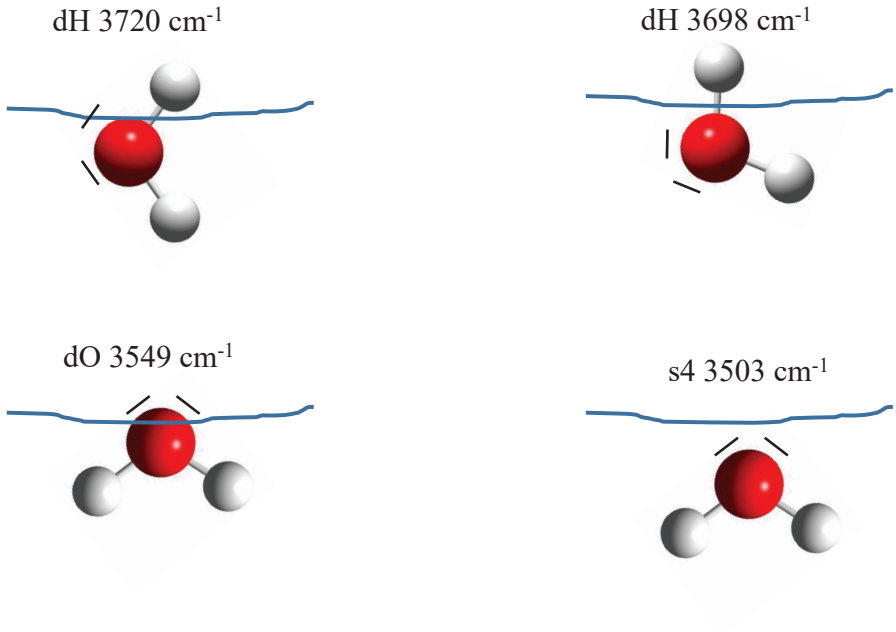

Figure 1: Four types of dangling modes of ASW.

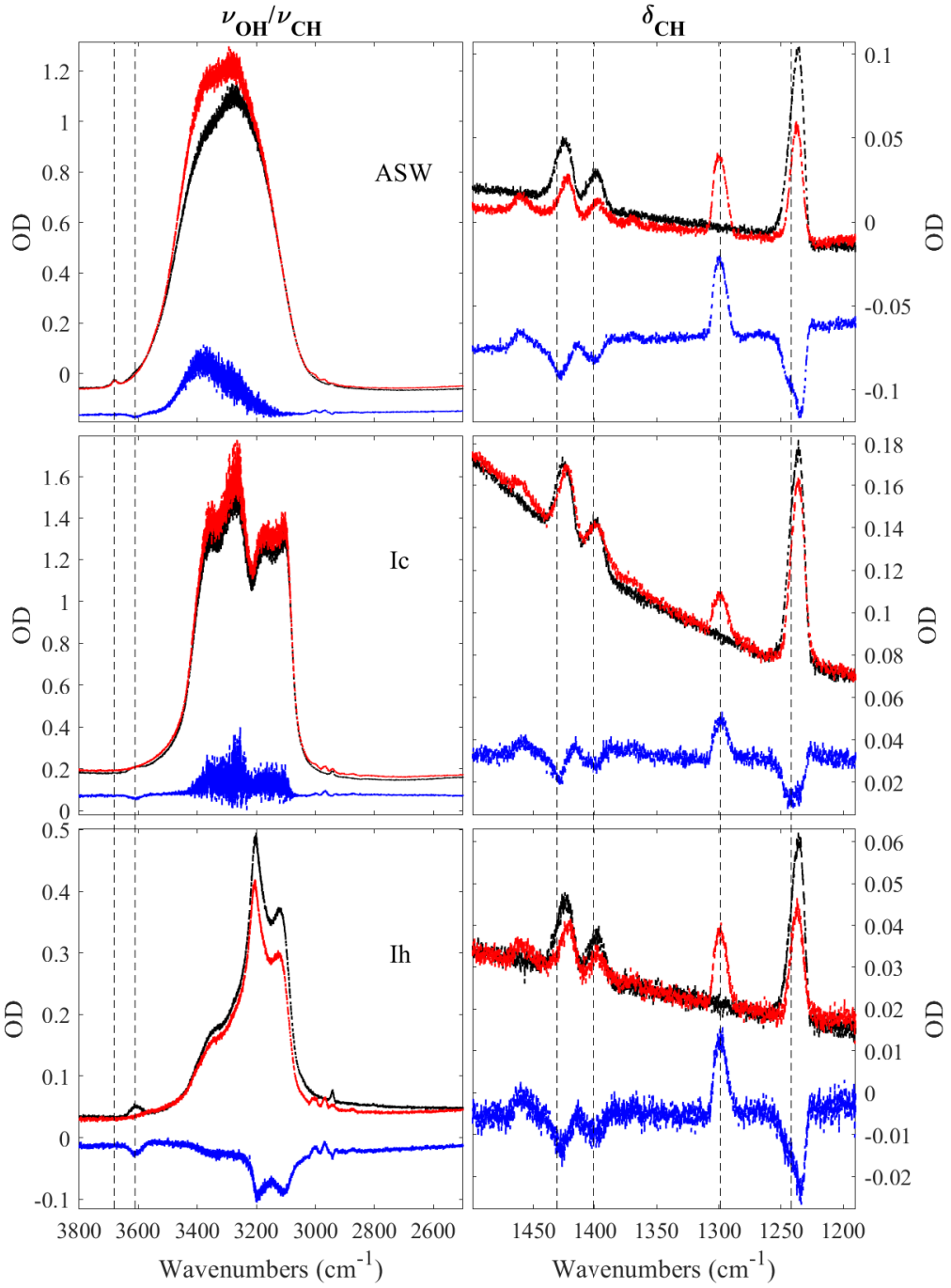

Figure 2: OH/CH stretching and CH bending regions of CH_3I adsorbed on amorphous (top), cubic (medium) and hexagonal (bottom) water ices, at 4.3 K, respectively. Dashed lines are located at 3682, 3607, 1431, 1401, 1298.8 and 1241.8 cm^{-1}, respectively. Black spectra: spectra after deposition at 20 K; red spectra: top: 60 min of irradiation using a $\lambda > 290$ nm filter, then 70 min without filter, average power 600 W; medium: after 210 min of irradiation using a $\lambda > 290$ nm filter, then 30 min without filter, average power 600 W; bottom: 150 min of irradiation using a $\lambda > 290$ nm filter, then 70 min without filter, average power 600 W; blue spectra: difference spectra: (after - before) irradiation.

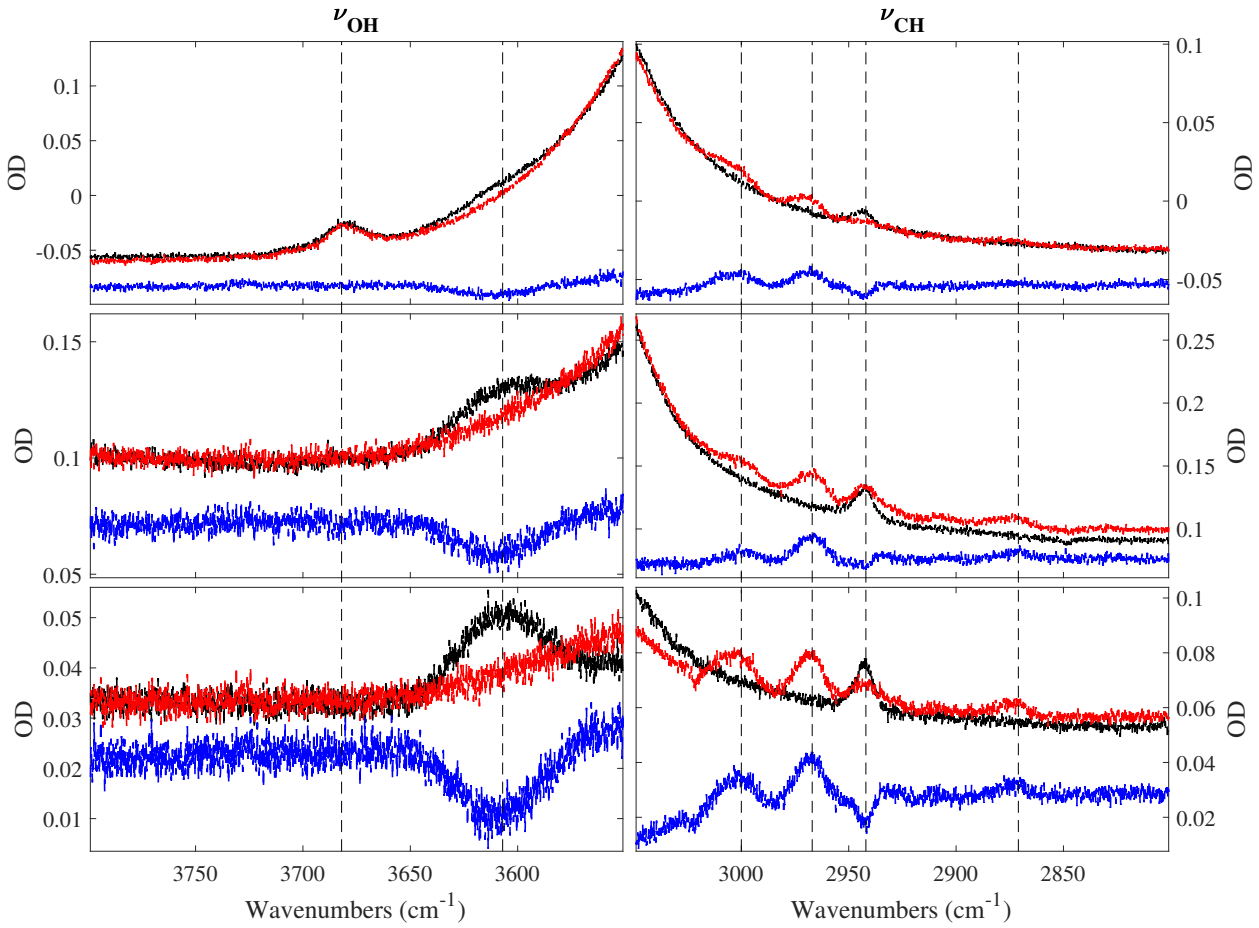

Figure 3: OH/CH stretching region of CH_3I adsorbed on amorphous (top), cubic (medium) and hexagonal (bottom) water ices, recorded at 4.3 K (for deposition details, please see experimental part). Dashed lines are located at 3682, 3607, 3000, 2967, 2942 and 2871 cm^{-1}, respectively. Black spectra: spectra after CH_3I adsorption (please see experimental part); red spectra: top: after 210 min of irradiation using a $\lambda > 290$ nm filter, then 90 min without filter, average power 600 W; medium: after 210 min of irradiation using a $\lambda > 290$ nm filter, then 30 min without filter, average power 600 W; bottom: 90 min of irradiation using a $\lambda > 290$ nm filter, then 120 min without filter, average power 600 W; blue spectra: difference spectra: (after - before) irradiation.

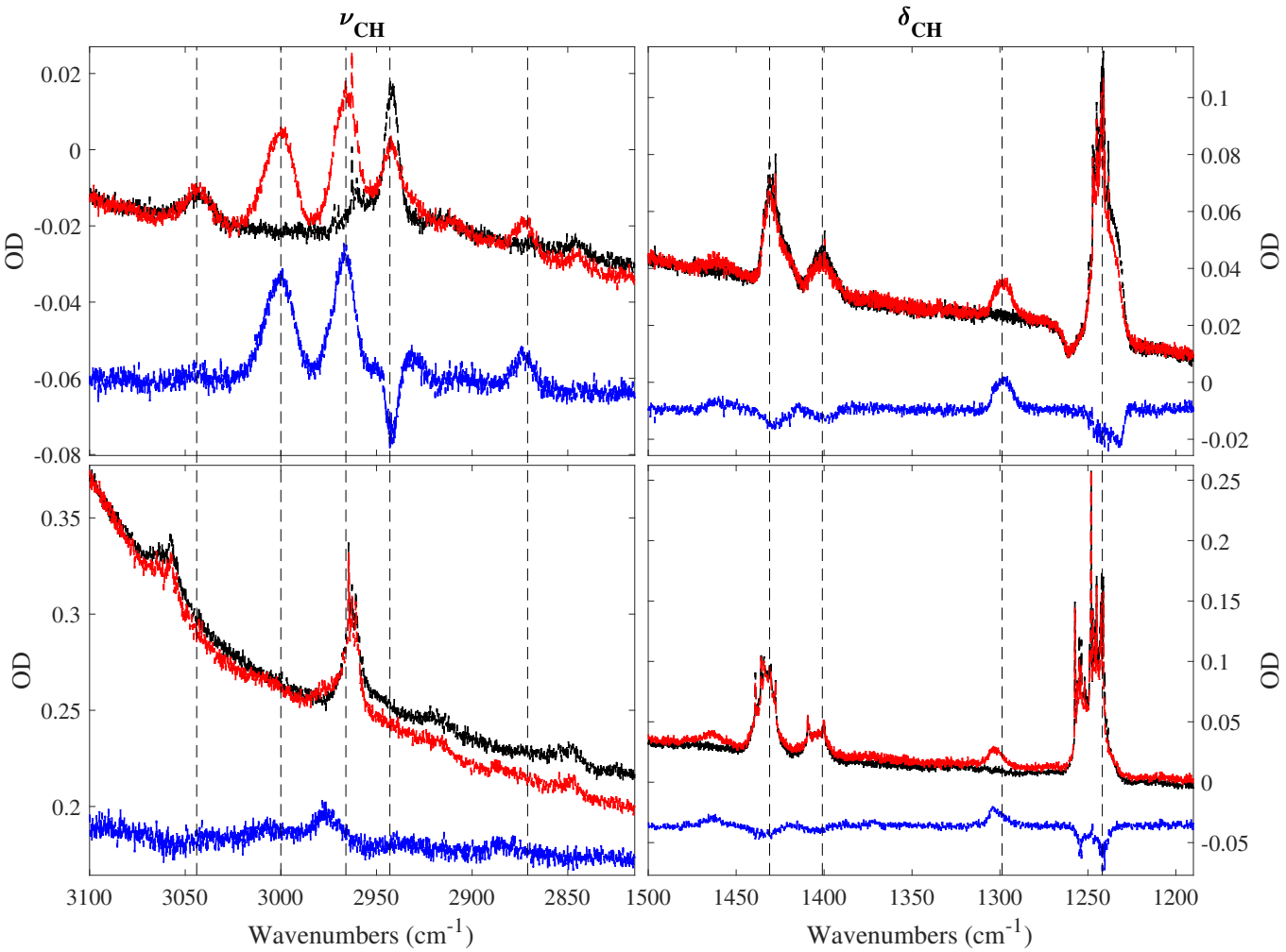

Figure 4: ν_{CH} and δ_{CH} of CH_3I trapped in Ar (top spectra), and of CH_3I...H_2O mixture trapped in Ar (bottom spectra), at 4.3 K, respectively. Dashed lines are located at 3044, 3000, 2966, 2943, 2871, 1431, 1401, 1298.8 and 1241.8 cm^{-1}, respectively. Black spectra: spectra after deposition at 20 K; red spectra: top: 60 min of irradiation using a $\lambda > 290$ nm filter, then 70 min without filter, average power 600 W; bottom: 150 min of irradiation using a $\lambda > 290$ nm filter, then 70 min without filter, average power 600 W; blue spectra: difference spectra: (after - before) irradiation.

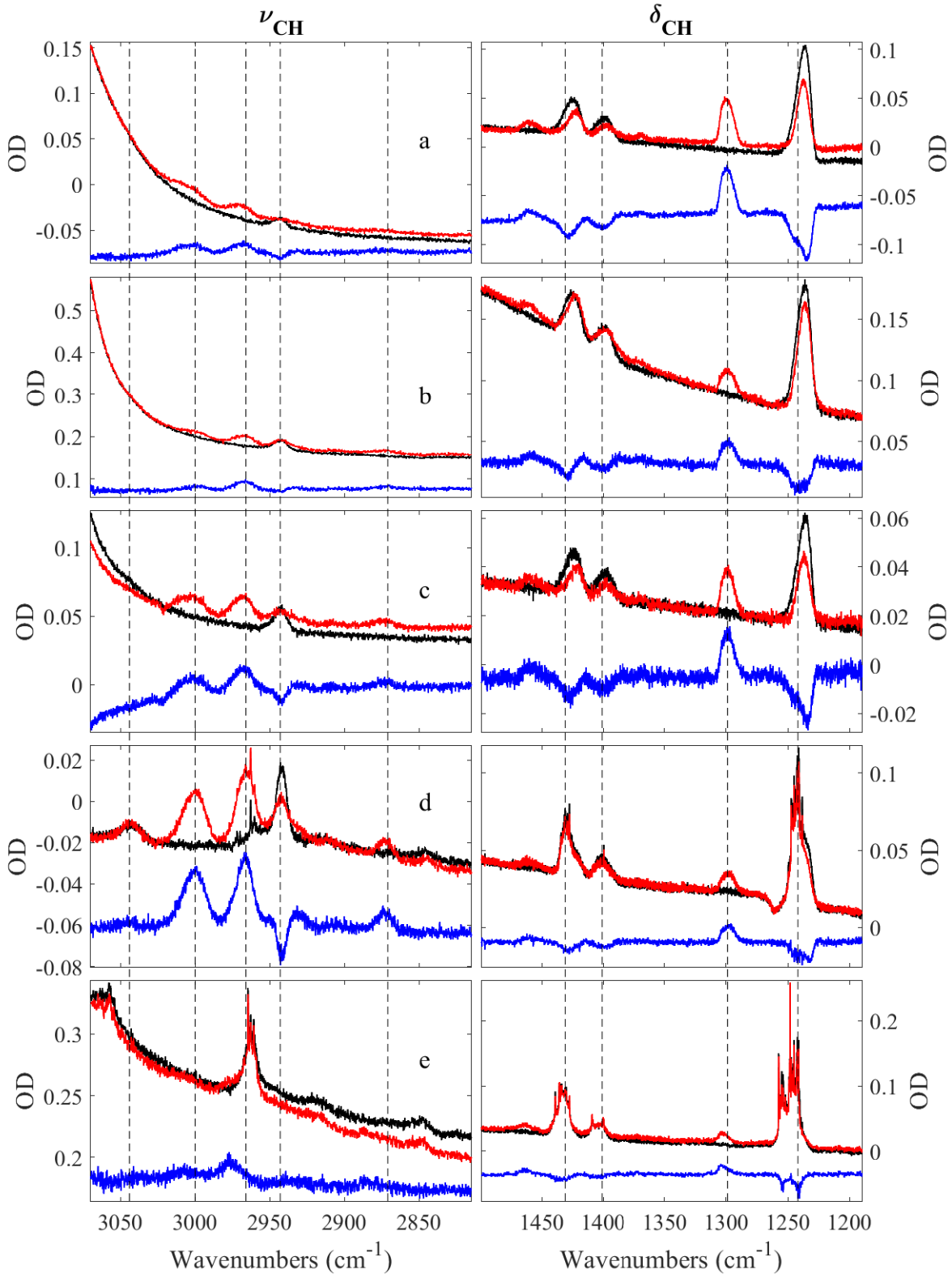

Figure 5: Comparison between CH_3I trapped on the surface of ASW (a), Ic(b), Ih(c), CH_3I in argon matrix (d), and CH_3I...H_2O mixture (e). For details, please read captions of Figure 2. Dashed lines are located at 3044, 3000, 2966, 2943, 2871, 1431, 1401, 1298.8 and 1241.8 cm^{-1}, respectively.

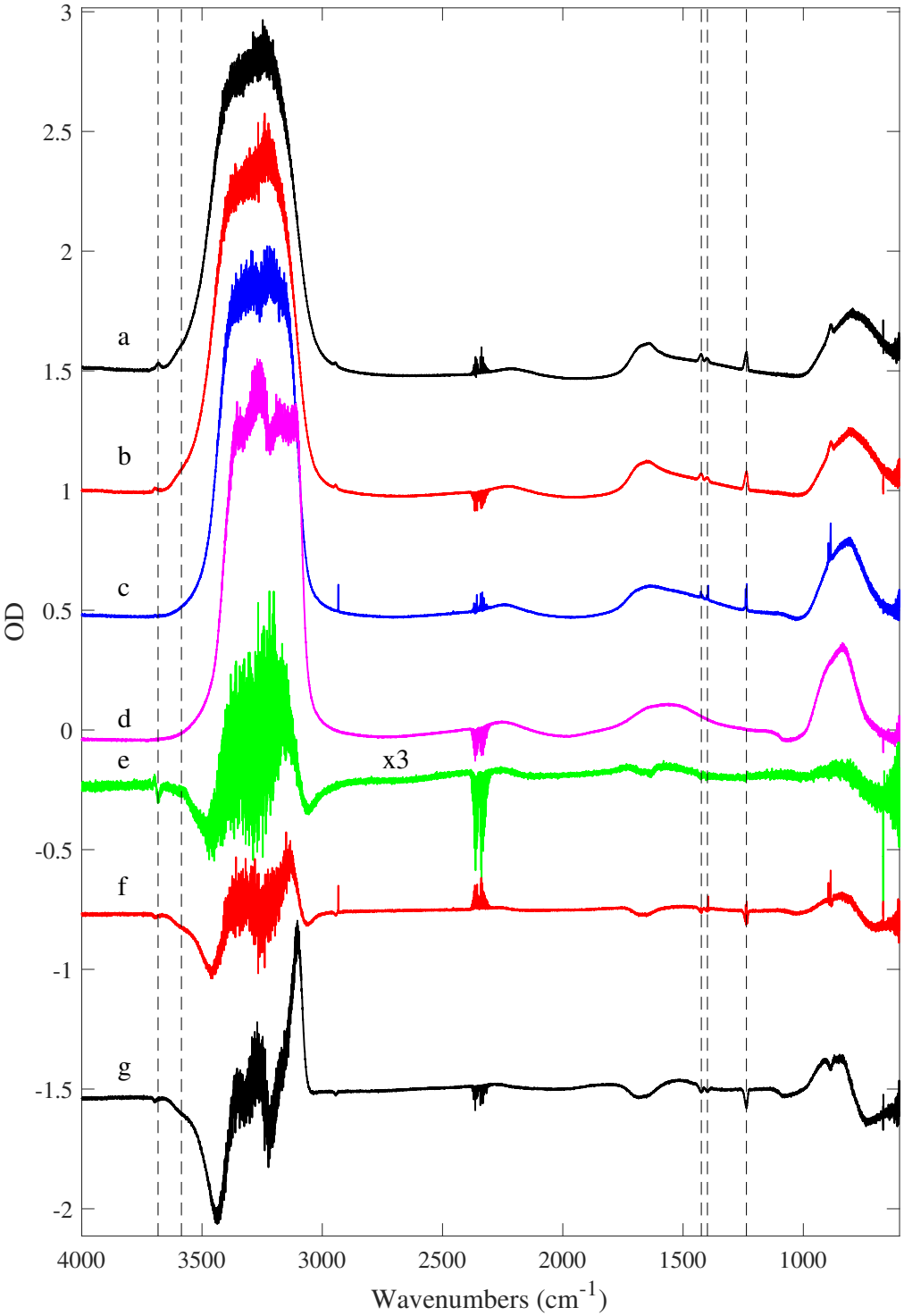

Figure 6: Annealings of iodomethane trapped on ASW. All the spectra have been recorded at 4 K (for experimental details, see experimental part). (a): spectrum after CH_3I deposition; (b): spectrum after annealing to 70 K; (c): spectrum after annealing to 130 K; (d): spectrum after annealing to 150 K; (e): (b-a)×3; (f): (c-a); (g): (d-a). Dashed lines are located at 3682.7, 3585.6, 1424.1, 1398.7 and 1236.6 cm^{-1}, respectively. The two first are linked to dH, dO and s4 modes, while the three latter are linked to CH_3I.

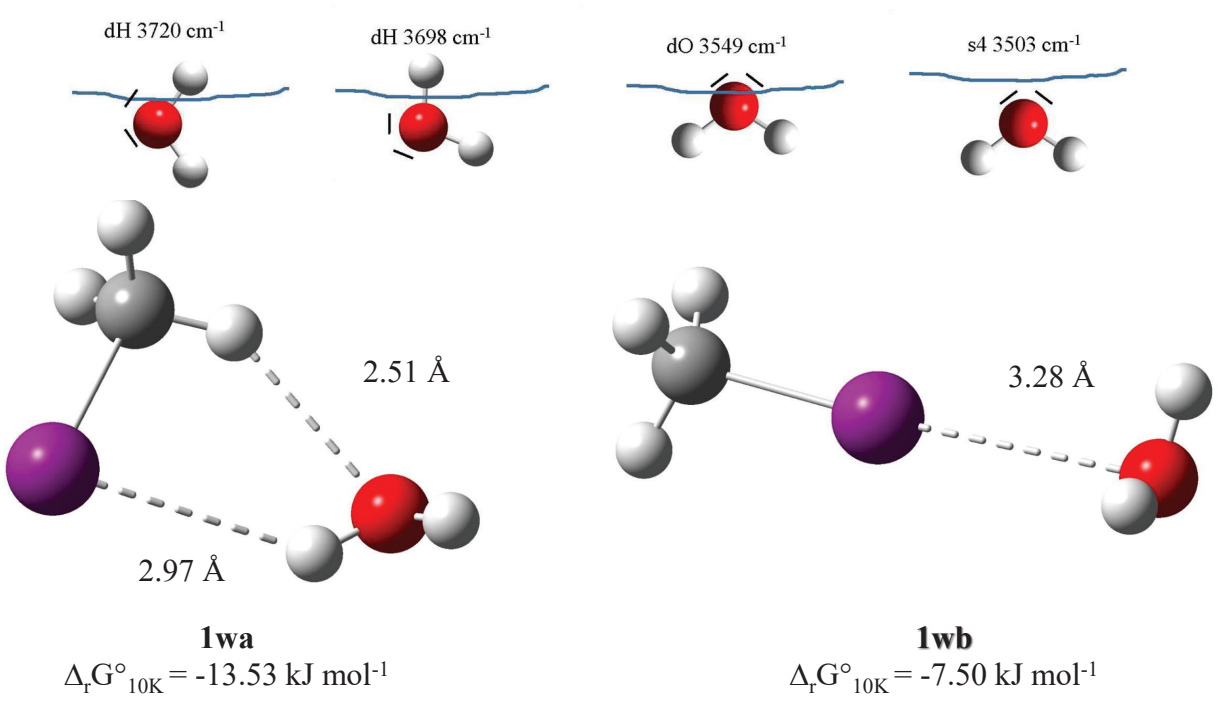

Figure 7: The two most stable hetero-dimers $CH_3I...H_2O$ calculated at the ωB97X-D/aug-cc-pVTZ(O,C) and aug-cc-pVTZ-PP(I) level of theory[36] together with illustration of the four dangling modes of ASW.

References

(1) Sherwen, T.; Evans, M. J.; Carpenter, L. J.; Schmidt, J. A.; Mickley, L. J. Halogen Chemistry Reduces Tropospheric O_3 Radiative Forcing. *Atmos. Chem. Phys.*, **2017**, *17*, 1557-1569.

(2) Saiz-Lopez, A.; Lamarque, J.-F; Kinnison, D. E.; Tilmes, S.; Ordóñez, C.; Orlando, J. J.; Conley, A. J.; Plane, J. M. C.; Mahajan, A. S.; Sousa Santos, G.; Atlas, E. L.; Blake, D. R.; Sander, S. P.; Schauffler, S.; Thompson, A. M.; Brasseur. Estimating the Climate Significance of Halogen-driven Ozone Loss in the Tropical Marine Troposphere. *Atmos. Chem. Phys.*, **2012**, *12*, 3939-3949.

(3) Sherwen, T.; Schmidt, J. A.; Evans, M. J.; Carpenter, L. J.; Großmann, K.; Eastham, S. D.; Jacob, D. J.; Dix, B.; Keonig, T. K.; Sinreich, R.; Ortega, I.; Volkamer, R.; Saiz-Lopez, A.; Prados-Roman, A. S.; Mahajan, A. S.; Ordóñez, C. Global Impacts of Tropospheric Halogens (Cl, Br, I) on Oxidants and Composition in GEOS-Chem. *Atmos. Chem. Phys.*, **2016**, *16*, 12239-12271.

(4) O'Dowd, C. D.; Jimenez, J. L.; Bahreini, R.; Flagan, R. C.; Seinfeld, J. H.; Hämeri, K; Pirjola, L.; Kulmala, M.; Gerard Jennings, S.; Hoffmann, T. Marine Aerosol Formation from Biogenic Iodine Emissions. *Nature*, **2002**, *417*, 632-636.

(5) Sipilä, M.; Sarnela, N.; Jokinen, T.; Henschel, H.; Junninen, H.; Kontkanen, J.; Richters, S.; Kangasluoma, J.; Franchin, A.; Peräkylä, O.; Rissanen, M. P.; Ehn, M.; Vehkamäki, H.; Kurten, T.; Berndt, T.; Petäjä, T.; Worsnop, D.; Ceburnis, D.; Kerminen, V.-M.; Kulmala, M.; O'Dowd, C. Molecular-scale Evidence of Aerosol Particle Formation via Sequential Addition of HIO_3. *Nature*, **2016**, *537*, 532-534.

(6) Baccarini, A.; Karlsson, L.; Dommen, J.; Duplessis, P.; Vüllers, J.; Brooks, I. M.; Saiz-Lopez, A.; Salter, M.; Tjernström, M.; Baltensperger, U.; Zieger, P.; Schmale, J.

Frequent new Particle Formation over the High Arctic Pack Ice by Enhanced Iodine Emissions. *Nat. Comm.*, **2020**, *11*, 4924.

(7) Fairbrother, D.H.; Briggman, K.A.; Stair, P.C.; Weitz, E. The Role of Adsorbate Structure in the Photodissociation Dynamics of Adsorbed Species: Methyl Iodide/MgO(100). *J. Chem. Phys.*, **1995**, *102*, 7267-7276.

(8) Calvert, J.G. Glossary of Atmospheric Chemistry Terms. *Pure Appl. Chem.*, **1990**, *62*, 2167-2219.

(9) Sohn, Y.; White, J.M. Thermal and Photochemistry of Methyl Iodide on Ice Film Grown on Cu(111). *Bull. Korean Chem. Soc.*, **2009**, *30*, 1470-1474.

(10) Miller, E.R; Muirhead, G.D.; Jensen, E.T. Mechanisms for the Near-UV Photodissociation of CH_3I on D_2O/Cu(110). *J. Chem. Phys.*, **2013**, *138*, 084702.

(11) Macdonald, M.L.; Wadham, J.L.; Young, D.; Lunder, C.R.; Hermansen, O.; Lamarche-Gagnon, G.; O'Doherty, S. Consumption of CH_3Cl, CH_3Br, and CH_3I and Emmision of $CHCl_3$, $CHBr_3$, and CH_2Br_2 from the CFForefield of a Retreating Artic Glacier. *Atmos. Chem. Phys.*, **2020**, *20*,7243-7258.

(12) Mahajan, A.S.; Shaw, M.; Oetjen, H.; Hornsby, K.E.; Carpenter, L.J.; Kaleschke, L.; Tian-Kunze, X.; Lee, J.D.; Moller, A.J.; Edwards, P.; Commane, R.; Ingham, T.; Heard, D.E.; Plane, J.M.C. Evidence of Reactive Iodine Chemistry in the Artic Boundary Layer. *J. Geophys. Res.*, **2010**, *115*,D20303.

(13) Atkinson, H.M.; Hughes, C.; Shaw, M.J.; Roscoe, H.K.; Carpenter.L.J.; Liss, P.S. Halocarbons Associated with Artic Sea Ice. *Deep-Sea Research I*, **2014**, *92*, 162-175.

(14) Li, C-X.; Chen, K.; Sun, X.; Wang, B-D.; Yang, G-P.; Li, Y.; Liu, L. Occurrence, Distribution, and Sea-Air Fluxes of Volatile Halocarbons in the upper Ocean off the

Northern Antarctic Penicula in Summer. *Science of the Total Environment*, **2021**, *758*, 143947.

(15) Heumann, K.G. Determination of Inorganic Traces in the Clean Room Compartment of Antarctica. *Analytica Chimica Acta*, **1993**, *283*, 230-245.

(16) Reviewed by Carpenter, L. J. *et al.*, **2021**. Marine Iodine Emissions in a Changing World. *Proc.R.Soc.A477*, **2020**, 20200824.

(17) Koenig, T. K.; Volkamer, R.; Apel, E. C.; Bresch, J. F.; Cuevas, C. A.; Dix, B.; Eloranta, E. W.; Fernandez, R. P.; Hall, S. R.; Hornbrook, R. S.; Pierce, R. B.; Reeves, J. M.; Saiz-Lopez, A.; Ullmann, K. Ozone Depletion Due to Dust Release of Iodine in the free Troposphere. *Sci. Adv.*, **2021**, *7*, eabj6544.

(18) Swanson, A.L.; Blake, N.J.; Dibb, J.E.; Albert, M.R.; Blake, D.R.; Rowland, F.S. Photochemically Induced Production of CH_3Br, CH_3I, C_2H_5I, Ethene, and Propene within Surface Snow at Summit, Greenland. *Atmospheric Environment*, **2002**, *36*, 2671-2682.

(19) Domine, F. Should We Not Further Study the Impact of Microbial Activity on Snow and Polar Atmospheric chemistry? *Microorganims*, **2019**, *7*, 260.

(20) Calvert, J. G. Glossary of Atmospheric Chemistry Terms. *Pure Appl. Chem*, **1990**, *62*, 2167-2219.

(21) DeSimone, A. P.; Olanrewaju, B. O.; Grieves, G. A.; Orlando, T. Photodissociation of Methyl Iodide Adsorbed on Low-Temperature Amorphous Ice Surfaces. *J. Chem. Phys.*, **2013**, *138*, 084703.

(22) Li, G.; Shin, Y.K.; Hwang, H.J. State-to-State Reaction Dynamics of CH_3I Photodissociation at 304 nm. *J. Phys. Chem. A*, **2005**, *109*, 9226-9231.

(23) Alekseyev, A.B.; Liebermann, H.P.; Buenker, R.J. An Ab Initio Study of CH_3I Photodissociation. II. Transitions Moments and Vibrational State Control of the I^* Quantum Yields. *J. Chem. Phys.*, **2007**, *126*, 2341031-23410311.

(24) Powis, I.; Black, J.F. Rotational Population and Alignment of $CD_3(v = 0)$ Photofragments from the A-Band Excitation of Methyl-D_3 Iodide. *J. Phys. Chem.*, **1989**, *93*, 2461-2470.

(25) Gardiner, S.H.; Lipciuc, M.L.; Karsili, T.N.V.; Ashfold, M.N.R.; Vallance, C. Dynamics of the A-Band ultraviolet Photodissociation of Methyl Iodide and Ethyl Iodide *via* Velocity-Map Imaging with 'Universal' Detection. *PCCP*, **2015**, *17*, 4096-4016.

(26) Warne, E.M.; Downes-Ward, B.; Woodhouse, J.; Parkes, M.A.; Billshaw, D.; Springate, E.; Majchrzak, P.; Zhang, Y.; Karras, G.; Wyatt, A.S.; Chapman, R.T. Kirrander, A.; Minns, R.S. Photodissociation Dynamics of CH_3I Probed *via* Multiphoton Ionisation Photoelectron Spectroscopy. *PCCP*, **2019**, *21*, 11142-11149.

(27) Granfors A.; Ahnoff, M.; Mills, M.M.; Abrahamsson, K. Organic Iodine in Antartic Sea Ice: A Comparison between Winter in the Wedell Sea and Summer in the Admunsen Sea. *J. Geophys. Res. Biogeosci.*, **2014**, *119*,2276-2291.

(28) Manca, C.; Martin, C.; Roubin, P. Spectroscopic and Volumetric Characterization of a Non-Microporous Amorphous Ice. *Chem. Phys. Lett.*, **2002**, *364(3-4)*, 220-224.

(29) Martin, C.; Manca, C.; Roubin, P. Adsorption of Small Molecules on Amorphous Ice: Volumetric and FT-IR Isotherm Co-Measurements Part I. Different Probe Molecules. *Surf. Sci.*, **2002**, *502-503*, 275-279.

(30) Noble J.A; Martin C.; Fraser H.J.; Roubin P.; Coussan, S. IR Selective Irradiations of Amorphous Solid Water Dangling Modes: Irradiation vs Annealing Effects. *J. Phys. Chem. C*, **2014**, *118*, 20488-20495.

(31) Noble, J.A.; Martin, C.; Fraser, H. J.; Roubin, P.; Coussan, S. Unveiling the Surface Structure of Amorphous Solid Water via Selective Infrared Irradiation of OH Stretching Modes. *J. Phys. Chem. Lett.*, **2014**, *5*, 826-829.

(32) Coussan, S.; Roubin, P.; Noble, J.A. Inhomogeneity of the Amorphous Solid Water Dangling Bonds. *PCCP*, **2015**, *7*, 9429-9434.

(33) Coussan, S.; Noble, J.A.; Cuppen, H.; Redlich, B.; Ioppolo, S. IRFEL Selective Irradiation of Amorphous Solid Water: from Dangling to Bulk Modes. *J. Phys. Chem. A*, **2022**, *126*, 2262-2269.

(34) Srivastava, A.; Osgood, R.M. State-Resolved Dynamics of 248 nm methyl-iodide Fragmentation on GaAs(110). *J. Chem. Phys.*, **2003**, *119*, 10298-10306.

(35) Jensen, E.T. Near-UV Photodissociation of Oriented CH_3I on Cu(110)-I. *J. Chem. Phys.*, **2005**, *123*, 204709.

(36) Sobanska, S.; Houjeij, H.; Coussan, S.; Aupetit, C.; Taamalli, S.; Florent, L.; Cantrel, L.; Gregoire, A.C.; Mascetti, J. Infrared Matrix-Isolation and Theoretical Studies of Interactions between CH_3I and Water. *J. Mol. Struct.*, **2021**, 130342.

(37) Tonauer, C. M.; Fidler, L-R.; Giebelmann, J.; Yamashita, K.; Loerting, T. Nucleation and Growth of Crystalline Ices from Amorphous Ices. *J. Chem. Phys.*, **2023**, *158*, 141001.

(38) Esteves-López, N.; Coussan, S. UV Photochemistry of Pyridine-Water and Pyridine-Ammonia Complexes Trapped in Cryogenic Matrices. *J. Mol. Struct.*, **2018**, *1172*, 65-73.